Proceedings of the 15th International Conference on Manufacturing Systems – ICMaS
Published by Editura Academiei Române, ISSN 1842-3183

"Politehnica" University of Bucharest, Machine and Manufacturing Systems Department
Bucharest, Romania, 26–27 October, 2006

INTEGRATED CAE DEVELOPMENT OF PRECESSIONAL DRIVES USING AUTODESK INVENTOR PLATFORM

**Ion BOSTAN, Florin IONESCU, Valeriu DULGHERU,
George CONSTANTIN, Anatolie SOCHIREAN**

Abstract: *The paper presents the modeling and simulation of precessional drives designed in two variants capable of high transmission ratio and torque for one stage compact construction. The constructions were designed in Inventor and also as multi body systems in MotionInventor. The simulations of the drives provide information concerning positions, velocities, accelerations, point trajectories, forces and moments, energies, as well as contact forces at the contact between gear teeth and satellite teeth and other data concerning the system. The bearings of the two drives were modeled as multi body systems in SolidDynamics for defining an approach for studying the noise emission during running through simulation with possibility of extension to the contact between teeth.*

Key words: *precessional drives, 3D multi body model, simulation, noise modeling.*

1. INTRODUCTION

The diversity of beneficiaries' requirements concerning mechanical transmissions bring out the necessity of increasing the reliability, efficiency and decreasing the mass and dimensions of drives. It becomes more and more difficult to satisfy the mentioned requirements by updating partially the traditional transmissions. This problem can be solved by using new types of mechanical transmissions, namely planetary precessional transmissions.

The advantages of the precessional planetary transmissions [1] lead to important economic advantage in using such drives. Some of the advantages are:

- *high efficiency*, rating 96%, is due to the gearing use with convex-concave teeth profile;
- *wide range of transmission ratio* is from ±8.5 to ±3 599 in the drive with only one stage;
- *high portent capacity* is achieved by meshing with about 100% teeth couples simultaneously engaged;
- *compactness and reduced weight* – the specific weight of drives ranges from 0.022 to 0.05 kg/Nm.
- *high kinematic accuracy*;
- *high rating life*;
- *low level of noise and vibration* from 50 to 60 dB;
- *low moment of inertia* due to the peculiarities of the spherical motion of the planet pinion.

The engineering methods based on computer permitted to develop a new type of precessional transmissions with multi-couple meshed teeth, which, from the technological point of view, can be manufactured by means of a new method of processing conical teeth with convex-concave profile.

It appeared the necessity of elaboration of new profiles adequate to the sphero-spatial motion of the gears which would ensure high performances to the precessional transmission. Considering the necessity of achieving the transfer function continuity and gear multiplicity some objectives were taken into account. One of them is the integrated methods of design, modelling and simulation using powerful means of creation and management of parametrical models of the mechanical assemblies on the basis of CAD-CAE platforms [4, 8] (Fig. 1).

The paper presents some original results of the activity in the frame of a project for developing two types of precessional drives with the characteristics transfer ratio, input speed, output torque respectively:

- i =100, n = 1 480 rot/min; M = 4.690 Nm;
- i =78, n = 1 480 rot/min; M = 1.480 Nm.

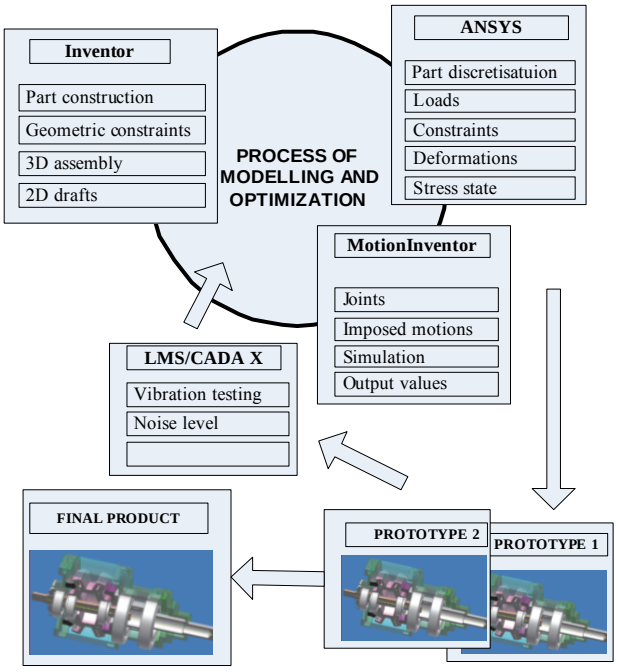

Fig. 1. Process of developing the precessional drive products using CAD-CAE platform.

2. KINEMATIC ANALYSIS AND PRECESSIONAL GEAR PROFILE TOOTH DEFINITION

2.2. Theoretical calculation of kinematic parameters of planetary precessional transmission

The planetary precessional transmission presented in Fig. 2 is the new transmission. Before modeling and simulation of this transmission some basic parameters are necessary to be calculated. In Fig. 2,*a* the kinematical scheme of planetary precessional transmission is shown, and in Fig. 2,*b* the 3D model of planetary precessional transmission is presented.

The main elements of the transmission are as follows: crankshaft 1 (*H*), block satellite 2 (*g*), fixed wheel gear 3 (*b*), and mobile wheel gear 4 (*a*). The advantage of the drive is that having such a design it is possible to obtain a transfer ratio up to 3600, and using designs with double-stage the transfer ratio of the mechanism can reach the value of 15 000 000. It is obvious that having such high transfer ratio there are big loads on the gear teeth. This problem is solved by the participation of all teeth in meshing, the load being distributed to half of them.

The functioning principle [1, 7] of the planetary precessional transmission is the following: the crankshaft 1, by means of the inclined section, is bearing a block satellite 2 with spatially spherical movement; the block satellite, by means of a crown with conical rollers instead of teeth, interacts with a fixed gear 3 on one side and on the opposite side another crown with conical rollers is in contact with the gear 4. The two gears have a special tooth profile defined by means of the motion equations. The mobile gear 4 is fixed on the output shaft of reducer, transferring to it the torque moment and revolution speed. The directions of rotation of input and output shafts can be the same or opposite. One can ascertain that when calculating the transfer ratio if it is a positive number there exist identical rotations for input and output shafts.

The transfer ratio of the planetary precessional transmission is defined by relation [3]:

$$i = -\frac{Z_{g_1} Z_a}{Z_b Z_{g_2} - Z_{g_1} Z_a}, \qquad (1)$$

where: Z_{g1}, Z_{g2} are number of rollers of the satellite crowns g_1 and g_2; Z_a and Z_b are number of teeth of the gears *a* and *b*.

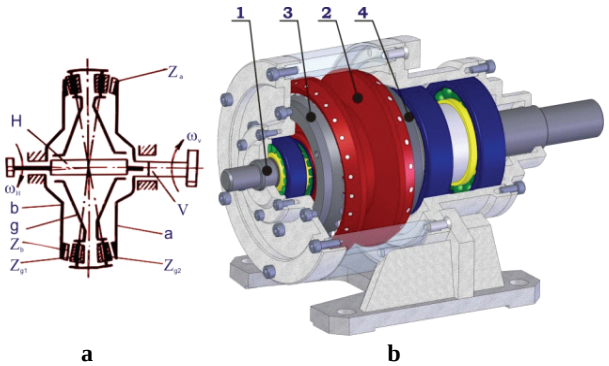

a **b**

Fig. 2. Model of planetary precessional transmission: *a* – kinematic diagram; *b* – 3D assembly.

The definition of dynamic loadings in the bearings *A*, *B* between crankshaft and drive housing, and *D*, *E* between crankshaft and block satellite (Fig. 3) is very important for the planetary precessional transmission. The bearings *A*, *B* (inner rings) rotate with input speed and are loaded with a complex loading (radial-axial). Therefore, in this node tapered roller bearings are used (Fig. 3), which have high loading capacity at small dimensions. The sizes of bearings (in particular external diameter) are imposed by the size of a gear with rollers of the block satellite. In the points *D* and *E* the roller bearings with a possibility of axial motion for auto-positioning (self finding its centre) of the block satellite between fixed and mobile gears are chosen.

For the theoretical calculation of dynamic loadings in points *A*, *B*, *D*, *E* (Fig. 3) the dynamic model of motion transfer (Fig. 4) was created.

According to Euler theory, the fixed frame of coordinates $OX_1Y_1Z_1$, and mobile system of coordinates *OXYZ* rigidly connected with the block satellite 1 are located according to the scheme shown in Fig. 3. For the given example we suppose that the centre of gravity is situated in point *O*, the center of precession.

In the scheme shown in Fig. 4, all values which define the dynamic reactions in the bearings of the block satellite revolving on the crankshaft in points *D*, *E*, and of crankshaft revolving on housing in points *A*, *B* are shown [2].

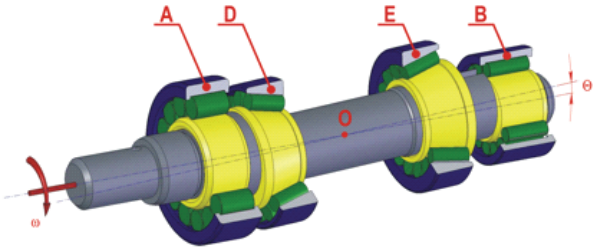

Fig. 3. Base bearings of planetary precessional transmission.

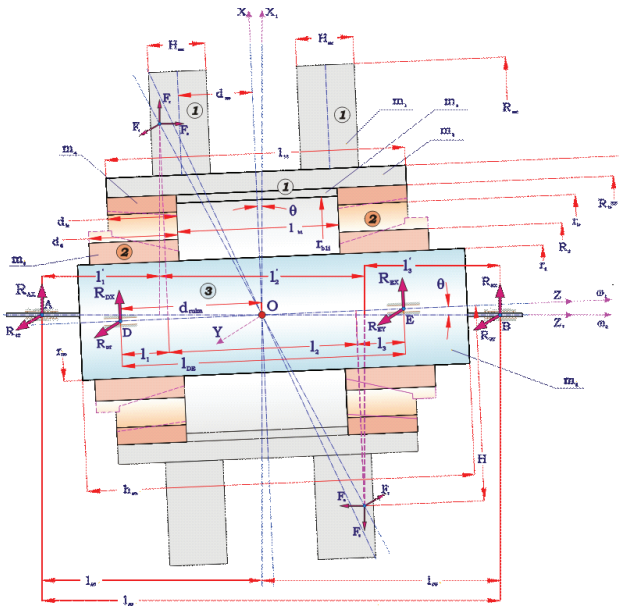

Fig. 4. Dynamic model of planetary precessional transmission.

The static loads are determined depending on the forces of gearing: axial force F_a, radial force F_r and a tangential force F_t, and the distances between them.

For defining the dynamic loadings, we take in consideration that they depend on geometry of the mechanism, motion characteristic and speed. In this case, there is an important factor which is necessary to be established, namely the limit of speed up to which the transmission is possible to work, in view of loading in bearings.

The description of dynamics of the block satellite is performed by means of Euler dynamic equations for movement of rigid body about of a motionless point:

$$\begin{aligned}
&\frac{dL_X}{dt}+\omega_{2Y}L_Z-\omega_{2Z}L_Y=M_X^{(e)},\\
&\frac{dL_Y}{dt}+\omega_{2Z}L_X-\omega_{2X}L_Z=M_Y^{(e)},\\
&\frac{dL_Z}{dt}+\omega_{2X}L_X-\omega_{2Y}L_X=M_Z^{(e)},
\end{aligned} \tag{2}$$

where: ω_{2X}, ω_{2Y}, ω_{2Z} and L_X, L_Y, L_Z are projections of angular speed and the linear momentum for each axis respectively, which will be $\omega_{2X}=\omega_2\sin\theta$; $\omega_{2Y}=0$; $\omega_{2Z}=\omega_2\cos\theta-\omega_1$; $L_X=I_X\omega_{2X}$; $L_Y=I_Y\omega_{2Y}$; $L_Z=$ $=I_Z\omega_{2Z}$; $M_X^{(e)}$; $M_Y^{(e)}$; $M_Z^{(e)}$ – projections of the moments of external forces on axes.

After a series of transformations, we obtain the definition relation for dynamic loading in points D and E:

$$Q_D=Q_E=\frac{M_Y^{(e)}}{l_{DE}}=\frac{\omega_2\sin\theta\left[I_Z\omega_1+\omega_2\cos\theta(I_X-I_Z)\right]}{l_{DE}}, \tag{3}$$

where I_X and I_Z are the total moments of inertia on axis X and Z respectively; ω_2 – angular speed of the block satellite concerning a mobile axis.

The definitions of additional dynamic loads in bearings A and B, which appear as a result of the dynamic unbalance of the inclined part of crankshaft, are as follows:

$$\begin{aligned}
&Q'_{AX_1}+Q'_{BX_1}=0\\
&Q'_{AY_1}+Q'_{BY_1}=0\\
&\frac{1}{2}l_{AB}Q'_{AY_1}-\frac{1}{2}l_{AB}Q'_{BY_1}=-I_{YZ_1}\omega_2^2\\
&-\frac{1}{2}l_{AB}Q'_{AX_1}+\frac{1}{2}l_{AB}Q'_{BX_1}=I_{XZ_1}\omega_2^2,
\end{aligned} \tag{4}$$

where Q'_{AX_1}, Q'_{BX_1}, Q'_{AY_1}, Q'_{BY_1} are the projections of additional dynamic loads on the axes X_1 and Y_1 on inclined part of a crankshaft in points A, B; l_{AB} – distance between respective points; I_{XZ_1} and I_{YZ_1} – the moment of centrifugal force of inertia concerning respective axes.

After a series of transformations, considering the axis Y_1 as the main axis of inertia of the given segment and $I_{YZ_1}=0$, one obtains the following relation for the calculation of additional dynamic loads in points A and B:

$$-Q'_{AX_1}=Q'_{BX_1}=\frac{\omega_2^2}{2l_{AB}}\sin 2\theta(I_Z-I_X). \tag{5}$$

The total additional dynamic load is defined by relations:

$$\begin{aligned}
&Q_{AX_1}=Q'_{AX_1}+\frac{\omega_2\sin\theta\left[I_Z\omega_1+\omega_2\cos\theta(I_X-I_Z)\right]}{l_{DE}},\\
&Q_{BX_1}=Q'_{BX_1}+\frac{\omega_2\sin\theta\left[I_Z\omega_1+\omega_2\cos\theta(I_X-I_Z)\right]}{l_{DE}}.
\end{aligned} \tag{6}$$

3. CAE SIMULATION OF KINETO-STATIC PARAMETERS OF PLANETARY PRECESSIONAL TRANSMISSION

The calculation [5] of the planetary precessional transmission by simulation is carried out using the simplified 3D model created in program Motion Inventor 2004+ [10, 11] but from which it is possible to determine and verify dynamic loads in bearings which have been designed earlier.

The 3D model for calculation is shown in Fig. 5. It includes the crankshaft 1, fixed wheel 2, the block satellite 3, a mobile wheel 4 rigidly connected to the output shaft 5.

The dynamic model has been created on the basis of the 3D assembly model [8, 9]. As the initial data has been specified speed on input shaft in deg/sec and the moment of torsion on the output shaft in Nm.

The kinematic joints (Fig. 5) were inserted according to the required movements of the drive. The crankshaft is supported by the drive housing through cylindrical roller bearings, which means a connection through a cylindrical joint (R-T), which gives the possibility of satellite self-centering. The block satellite is mounted on the inclined part of the crankshaft by means of two conical roller bearings that require two joints of Point-Line type (R-R-T). The conical rollers are mounted on small shafts on the block-satellite, which means Revolution joints (R). The contact between the rollers of the block-satellite and the fixed and mobile wheel are modeled through 3D contacts of material couples (steel on steel). The output shaft having at one end the fixed mounted output wheel, is supported by the housing by means of two conical roller bearings, thus it has a revolution motion that leads to Revolution

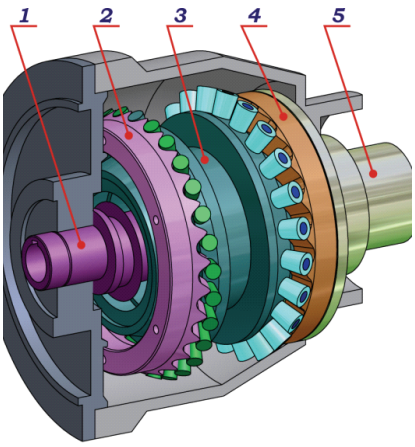

Fig. 5. 3D Model of planetary precessional transmission.

joint (R) in the model. The fixed wheel is attributed to the Base, which is always immobile and accompanied by the main coordinate frame. The model accompanied by the tree regarding the joints is shown in Fig. 6.

The model study was achieved in stages. In the first stage, the kinematic analysis was carried out, which included the following parameter simulations: transfer ratio, absolute angular speed of the block satellite, relative angular speed of the block satellite, angular speed on the output shaft. The obtained results are shown on Fig. 7. Some other important parameters were obtained, such as transfer ratios between different elements of the drive shown in Fig 8.

The next stage implied the kineto-static analysis with numerical calculation through simulation of total loadings in bearings of the block satellite on crankshaft. Some results of simulation are presented on Fig. 9.

In the shown diagrams the straight line stand for the total theoretical loading in points *C* and *D*. The second curve represents the variation of total loading in the same points obtained on the basis of numerical results of simulation.

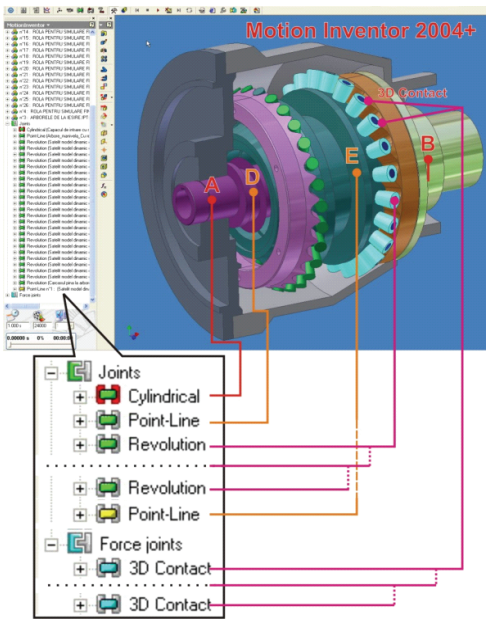

Fig. 6. Kinematics joints in the precessional transmission.

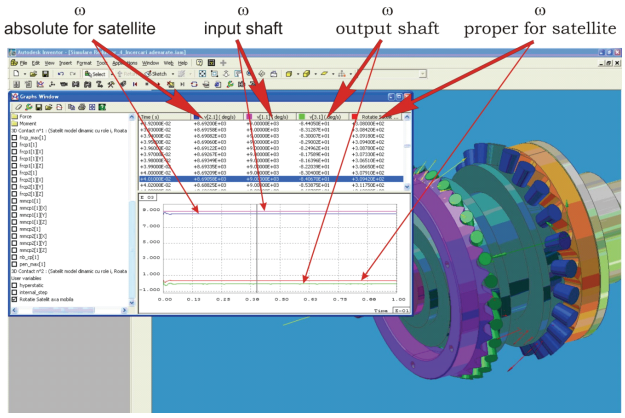

Fig. 7. Kinematic calculation of planetary precessional transmission.

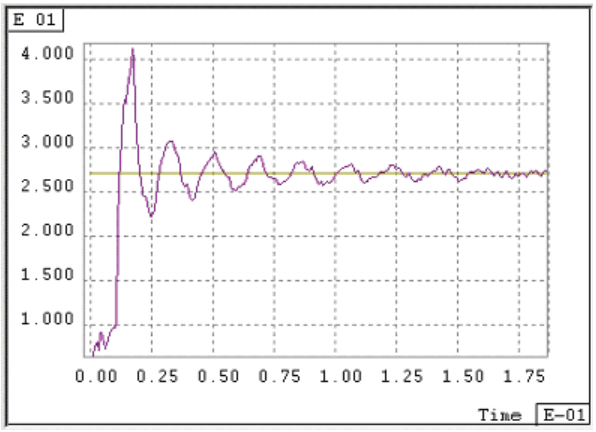

Fig. 8. Simulated transfer ratio between input shaft and satellite: theoretical - *isat_theo*; calculated – *isat_calc*.

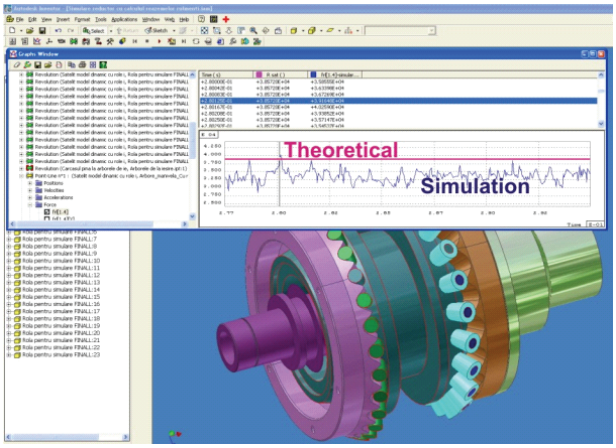

Fig. 9. Calculation of dynamic loadings in the bearings between the block satellite and crankshaft.

As a result of the simulations, the following important results have been obtained: the theoretical calculations have been confirmed and also opportunity of performing kineto-static calculations by computer, simulation and optimization of calculations by means of computer modelling have been proved using CAE programs, such as Motion Inventor 2004 + [10, 11].

During the third stage the additional dynamic reactions in crankshaft bearings supported by the reducer housing have been determined. The simulation data concerning the reaction are shown in Fig. 10.

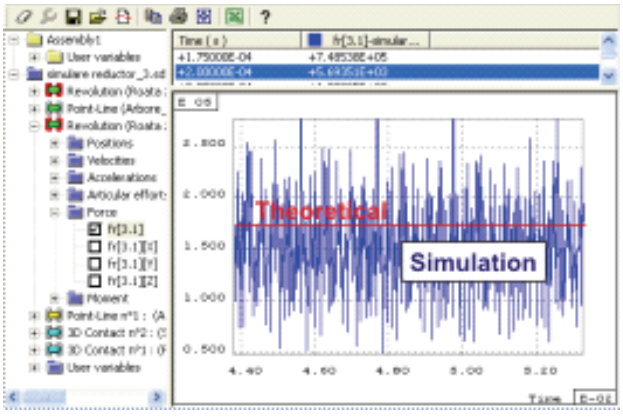

Fig. 10. Calculation of dynamic loadings in the bearings support between the crankshaft and cases of a reducer.

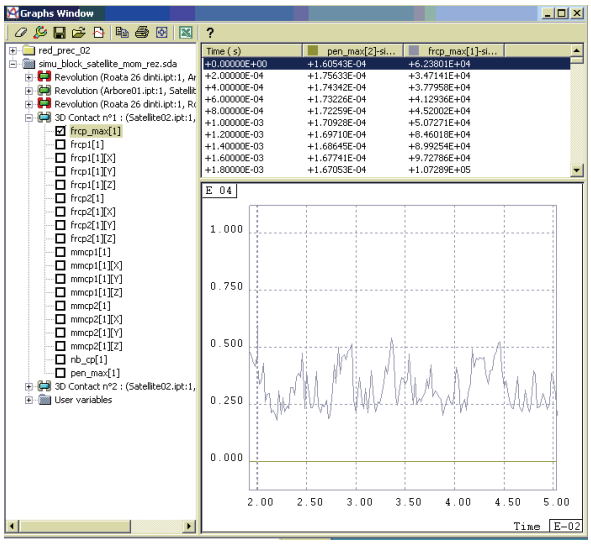

Fig. 11. Maximum of the contact forces in 3D contact joint fixed gear-satellite

The straight line shows the total theoretical reaction (static and dynamic) of the bearings of the couple satellite-inclined shaft, the second curve stands for the value of the same reaction calculated by means of CAE simulation.

Obviously, that as in the first case the theoretical data which have been specified earlier was determined and verified, a great opportunity of calculation of precessional transmission by computer simulation being opened.

Considering that the dynamic reactions depend to a great extent on revolution speed, the analysis of the behavior of the block satellite with different revolution speeds was accomplished (Fig. 11). The bearing loadings can increase two-three times and even more at high speeds. By performing such an analysis, it is possible to define precisely a range of use of planetary precessional transmission, followed by the use of additional methods of minimization of dynamic loads.

In this study, the bearings of the output shaft were not considered, they being defined only with static loads due to output shaft revolution speed, which is much less than at the drive input.

4. ELEMENTS OF NOISE MODELLING AND SIMULATION IN PRECESSIONAL TRANSMISSIONS

During a vibratory motion of a mechanical system, the amount of energy which is transferred to the medium is dependent upon the amplitude of vibrations.

The energy gathered in a system and hence the amplitudes during a vibratory motion of a mechanical system are directly dependent on the work done to displace the mechanism elements. In our case there exist a Herzian contact between intermediary elements of the bearings and the ring races and also between gearing teeth. It has to be considered also the bending motion of the teeth in contact.

The energy being directly dependent of amplitude of vibration, thus more energy is transferred to the elastic medium. We are interested in the amount of energy transported through a certain area of the elastic medium per unit of time which is the intensity of the sound wave I. Knowing that the ratio between energy E and time t is equivalent to power, intensity I is the ratio between power and area A as follows:

$$I = \frac{E}{t \cdot A} \text{ or } I = \frac{P}{A}. \tag{5}$$

The elastic medium can propagate energy as a wave. It is more convenient to describe energy E passing any given point with respect to time t, which leads to power, the rate of energy flow being

$$P = \frac{E}{t} \text{ in W}. \tag{6}$$

A logarithmic scale to the base 10 is often appropriate due to large variations of power in typically applications. This leads to the definition of the power level as

$$\mathrm{d}B = 10\log\left(\frac{W}{W_{ref}}\right), \tag{7}$$

where W is power (in W) given with respect to a reference power W_{ref}.

The *Sound Power Level* L_w is used to describe the *acoustic power* from a source. This is a small percentage of the power driving the source. The power reference for L_w is of 10^{-12} W corresponding to the minimum acoustic power audible by a healthy adult. It is defined as:

$$L_W = 10\log\left(\frac{W}{10^{-12}}\right) \tag{8}$$

Energy dissipation mechanisms and influence factors. The sound is generated by a steady stream of energy with respect to time (*i.e.* power). It is generally considered that energy cannot be created or destroyed, only transformed. A proportion of energy input will be output as acoustic power, the rest being dissipated as heat. The total energy of the whole system can be described as:

$$E = \sum \Delta E_n + \sum \Delta E_f + \sum E_k + E_s + E_D, \tag{9}$$

where ΔE_n is the impact dissipation, ΔE_f is the friction dissipation, E_k is kinetic energy, E_s is kinetic energy of the primary system, and E_D is the dissipation by the primary damping.

Dissipation due to impact energy. We consider that τ is the contact period. The impact dissipation can be described as follows:

$$\Delta E_n = \int_0^{\tau} C_n(e,t)\, v_n^2(t)\, \mathrm{d}t. \tag{10}$$

Dissipation due to friction energy. When the tangential force F_t is greater than friction force F_f ($|F_t| > |F_f|$), there is relative sliding. Thus, the friction energy dissipation becomes

$$\Delta E_f = \int_0^{\tau} \mu_f F_n(t)\, v_t(t)\, \mathrm{d}t. \tag{11}$$

Deformation δ_k for point contact. When a force Q [N] is pressing two bodies of the same material on a contact point against each other, one obtains after Hertz

$$\delta_k = 1.5 \cdot \frac{2K}{\pi\mu} \frac{\left(1 - \frac{1}{m^2}\right)^2}{E \cdot a} Q \qquad \text{[mm].} \qquad (12)$$

For both bodies of steel with the elastic constant E = = 2.08 10^5 N/mm^2 and $1/m$ = 3/10, the expression can be simplified [6] as

$$\delta_k = \frac{2.79}{10^4} \cdot \frac{2K}{\pi\mu} \sqrt[3]{\sum \rho \cdot Q^2} \qquad \text{[mm].} \qquad (13)$$

Considering the deformation constant c_δ one can obtain

$$\frac{\delta_k}{D_w} = c_\delta \cdot \sqrt[3]{\left(\frac{Q}{D_w^2}\right)^2}, \qquad (14)$$

where D_w is the roller diameter and c_δ is obtained from the following relation

$$c_\delta = \frac{2.79}{10^4} \cdot \frac{2\kappa}{\pi\mu} \cdot \sqrt[3]{D_w \cdot \sum \rho} \qquad [(\text{N/mm}^2)^{-2/3}]. \qquad (15)$$

where κ is the osculation factor.

Deformation δ_k for linear contact. Given the fillet radius r of the cylindrical rollers and their length l_w, the effective contact length is

$$l_{eff} = l_w - 2r, \qquad (16)$$

where r is the roller fillet radius.

The deformation δ_k for linear contact cannot be calculated after Hertz. Bochmann determined empirically that the deformation δ_k depends on the first power of force Q [6]. In the late researches one can find the total deformation on both contact points of a roller with the races as double $\delta = 2\delta_k$, so

$$\delta = \frac{8.10}{10^5} \cdot \frac{Q^{0,925}}{l_{eff}^{0.85}} \qquad \text{[mm].} \qquad (17)$$

Modelling and simulation of bearings. Because a mathematical model is very difficult to achieve, it arose the necessity to use another method, namely the modeling and simulation of a mechanical system having elements in contact as a multi-body system. The Herzian contact stands for the noise modeling and simulation.

The contact simulation generates among other results the contact forces used for contact deformation simulation that stands for deformation energy determination.

The study was particularised for considering the modelling and simulation of bearings belonging to the drives. Three types of bearings were modelled as 3D assemblies (Fig. 12). For exemplification, the roller bearing (Fig. 12,*a*) is presented. The 3D model was enabled with kinematic and dynamic properties in MotionInventor program.

The following procedure of noise modelling and simulation was achieved for a roller bearing. In the MotionInventor model of the roller bearing we used the following joints (Fig. 13), after assembly creation in Inventor:

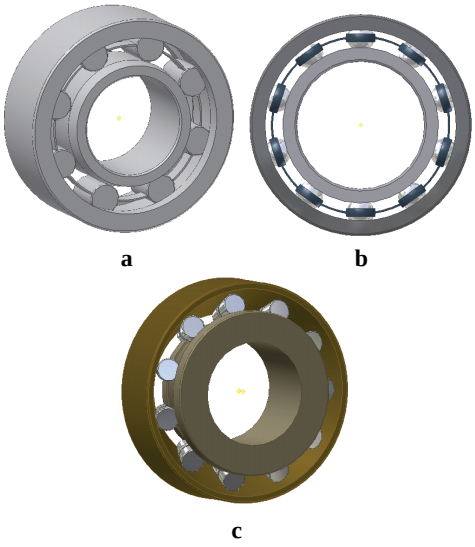

Fig. 12. 3D MotionInventor models of bearings: *a* – roller bearing; *b* – ball bearing; *c* – conical roller bearing.

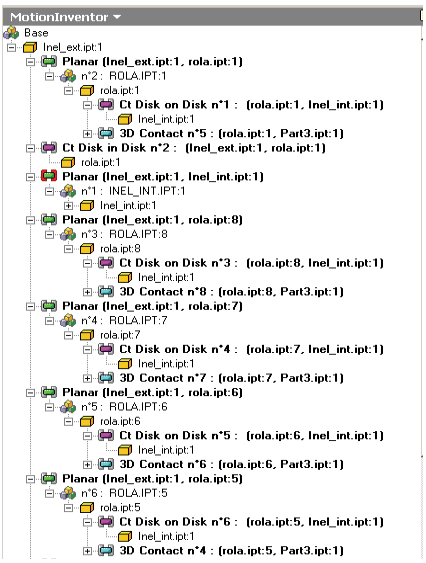

Fig. 13. Model tree of the roller bearing (MotionInventor).

- external ring – fixed on the Base (GROUNDED);
- internal ring – Planar joint (TTR);
- roller – Planar joint (TTR);
- separator – Revolution (in regard with inner ring):
- contact disc in disc (Herzian) between roller and external ring;
- contact disc on disc (Herzian) between roller and internal ring;
- contact – 3D Contac between roller and separator.

The contact forces between roller and external ring obtained in MotionInventor are used to calculate the followings:

- contact deformation of the roller (def_rol08);
- deformation variation (delta_ def_rol08);
- variation of time (step time) (delta_time);
- deformation speed (vit_def_rol08);
- (vit_def_rol08)^2:
- c*(vit_def_rol08)^2;
- dissipated energy c*(vit_def_rol08)^2*delta_time;

- deformation energy:force*vit_def_rol08*delta_time
- total dissipated energy: sum of dissipated energies on each step;
- total deformation energy: sum of deformation energies on each step;
- difference between total dissipated energy and total deformation energy;
- pressure sound calculation.

After simulation we obtained the variation of force on roller almost triangular. This form would influence the form of energy diagram, which is an integral of the product *force* × *speed of deformation* as in relation

$$E_{def} = \int_{t_i}^{t_f} F(t) \cdot v_{\delta k}(t) \cdot \mathrm{d}t. \qquad (18)$$

So the integral is the aria of the graph $F(t) \cdot v_{\delta k}(t)$ which approximates a triangle.

Using the relation between power and energy $W = \frac{E}{t}$, then the power of deformation becomes

$$W_{def} = \frac{E_{def}}{t_f - t_i} \quad [\mathrm{W}]. \qquad (19)$$

The simulation of sound power using relation (8) was achieved for a frequency of the roller on the outer race $\nu_{out} = 9.58$ Hz and a frequency of the inner ring in regard with the exterior one of $\nu_r = 23.23$ Hz.

As one can see on the force diagram (one cycle) in Fig. 14, the effect of rollers is combined, so the area of the diagram is doubled, three rollers acting on the outer ring. The combined effect *ball-outer ring* (the term ball is generic for intermediary elements balls, rollers, conical rollers) is reflected in a new sound power value:

$$L_{W\,total\,outer\_ring} = 10 \log\left(\frac{2 \cdot W_{def}}{10^{-12}}\right) \quad [\mathrm{dB}]. \qquad (20)$$

Considering also the effect ball-inner ring which is similar to that of ball-outer ring the sound power on the bearing is

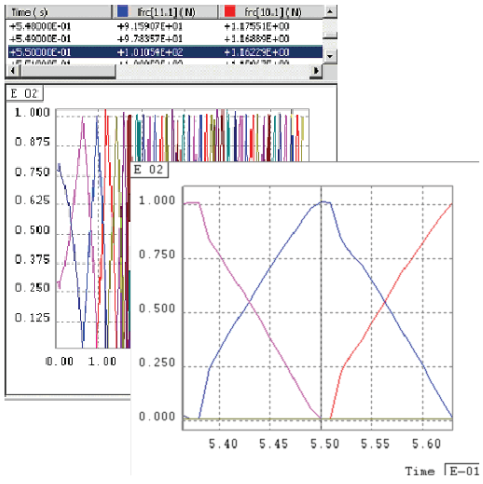

Fig. 14. Contact force variation on eight rollers during simulation time and on one cycle.

$$L_{W\,total\,bearing} = 10 \log\left(\frac{4 \cdot W_{def}}{10^{-12}}\right) \quad [\mathrm{dB}]. \qquad (21)$$

Impact energy dissipation. We obtained form the simulation process the deformation contact force C_n (Fig. 15) and the deformation speed v_n (Fig 16) as a linear speed being the ratio between variations of C_n and time Δt. The impact energy dissipation calculation by relation (11) needs to obtain the product between the contact deformation force C_n and the squared deformation speed v_n^2 (Fig. 17).

The total energy dissipation on inner and outer ring is $2 \times 2.26 \times 10^{-7}$ J. Considering the energy dissipation, the sound power on bearing is

$$L_{W\,total\,bearing} = 10 \log\left(\frac{4W_{def} - W_{dis}}{10^{-12}}\right) \quad [\mathrm{dB}]. \qquad (22)$$

It was obtained for a roller cycle a pressure sound of

$$L_W = 10 \log\left(\frac{W_{def}}{10^{-12}}\right) = 66 \quad [\mathrm{dB}]. \qquad (23)$$

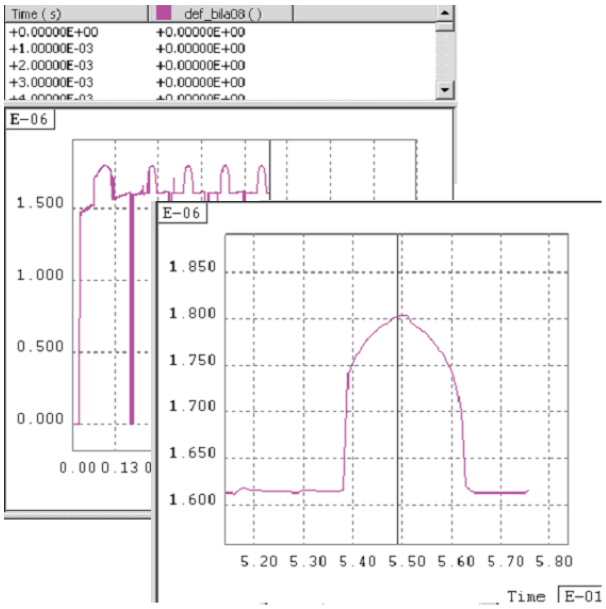

Fig. 15. Roller deformation during simulation time and on one cycle (enlarged image).

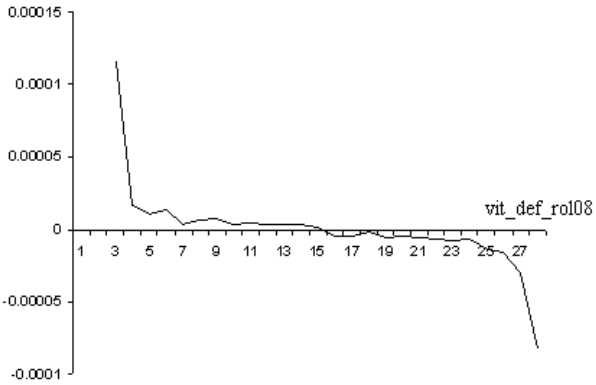

Fig. 16. Deformation speed over a contact cycle (Excel).

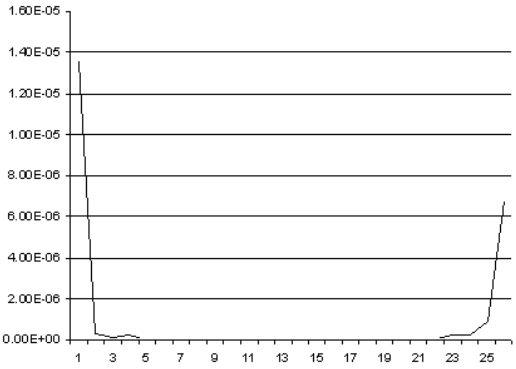

Fig. 17. Product $C_n v_n^2$ (Excel).

Adding the influence of different sources to the total noise. Supposing we have *n* sources of noise, each of them having a sound power level $\mathrm{d}B_n$, the total sound power level of the sources is given by the formula

$$\mathrm{d}B_1 + \mathrm{d}B_2 + \ldots + \mathrm{d}B_n = \\ = 10\log(10^{\mathrm{d}B1/10} + 10\mathrm{d}^{B2/10} + \ldots + 10^{\mathrm{d}Bn/10}). \quad (24)$$

The sound power could incorporate also the effects of tooth contact, which are cumulated but obviously not simply summated.

4. CONCLUSIONS

Among the characteristics of the estimated results of the research in the field of new and efficient drive development we can enumerate the followings:

- the precessional drives elaborated ensure: high portant capacity; high mechanical efficiency; high kinematic accuracy; low noise level and vibrations;
- new technologies of tooth processing achieved during this research ensure: high productivity; high manufacturing accuracy; low material consume; technological simplicity;
- costs of drives becomes more attractive as the costs of other equivalent drives.

The engineering methods achieved during the project will enable constructive optimization of the precessional planetary transmissions designed and argumentation of the restrictions regarding the real fields of utilisation of the precessional planetary transmissions.

The structural optimization of the precessional transmissions will allow synthesis of new schematics of precessional transmissions with constant and variable transmission ratio and elaboration of new schematics of precessional transmissions for specific running conditions.

REFERENCES

[1] Bostan, I. (1991). *Precessionnye Peredaci s Mnogoparnym Zacepleniem. Ştiinţa*, ISBN 5-376-01005-8, Chişinău.
[2] Bostan, I. (1992). *Precessional transmissions with multi-couple gear*, Edit. Ştiinţa, Chişinău.
[3] Bostan, I., Dulgheru, V., Grigoraş, Ş. (1997). *Planetary, precessional and harmonic transmissions*, Bucharest – Chişinău.
[4] Bostan, I., Cantemir, L., Ionescu, Fl. and V. Dulgheru. (2003). *Some Aspects of Creativity and Process and Product*, ARA-Journal, Volume 2000–2002, Nos. 25–26, ISBN 3-00-011583-8, pp. 136–138.
[5] Bostan, I., Ionescu, Fl., Dulgheru, V. and A. Sochireanu. (2004). *Kinetostatic Analysis of the Sphere – Spatial Mechanisms by using 3D-Models and -Simulations*, Meridian Ingineresc, Revue of the Technical University of Moldova and Moldavian Society of Engineers, Nr. 2, ISSN 1683-853-X, pp. 59–61.
[6] Brändlein, J., (1998). *Wälzlagerpraxis: Handbuch für Berechnung und Gestaltung von Lagerung. Vereinigte Fachverlage*, Mainz.
[7] Dulgheru V. (1995). *Doctor Habilitat Thesis*, Technical University of Moldova, Chişinău.
[8] Ionescu, Fl., Constantin, G., Haszler, Fl. (1996). *Metodologii înalt integrate de proiectare asistată şi optimizare pentru construcţia de maşini*, TCMM, 15, Proceedings ICMaS 1996, Editura Tehnică, Bucharest, ISBN 973-31-0766-2, pp. 213–220.
[9] Ionescu, Fl., Choynovski, F. G. Constantin. (2003). *Modelling and Simulation of Solid Body Systems*, ARA-Journal, Volume 2000–2002, Nos. 25–27, American Romanian Academy of Arts and Sciences, ISBN 3-00-011583-8, pp. 150–157.
[10] *** (2004). *MotionInventor. Powerful 3D Mechanical Simulation Software*, Solid Dynamics SA, France. www.solid-dynamics.com.
[11] *** *Autodesk Inventor* – www.autodesk.com.

Authors:

Prof. Acad. Dr. Dr. H.C. mult. Ion BOSTAN, Rector, Technical University of Moldova, Chair of Theory of Mechanisms and Machine Elements, E-mail: bostan@mail.utm.md
Prof. Dr. Dr. H.C. Dr. H.C. Florin IONESCU, University of Applied Sciences Konstanz, Chair of Theory of Mechanisms and Machine Elements, E-mail: ionescu@htwg-konstanz.de
Prof. Dr. Eng. Valeriu DULGHERU, Head of Deparment, Technical University of Moldova, Chair of Theory of Mechanisms and Machine Elements, E-mail: dulgheru@mail.utm.md
Prof. Dr. Eng. George CONSTANTIN, "Politehnica" University of Bucharest, Machine and Production Systems Department, E-mail: geo@htwg-konstanz.de
Lecturer Eng. Anatolie SOCHIREAN, Technical University of Moldova, Chair of Theory of Mechanisms and Machine Elements, E-mail: salic@mail.utm.md